EAT-20, a Novel Transmembrane Protein With EGF Motifs, Is Required for Efficient Feeding in *Caenorhabditis elegans*

Yukimasa Shibata,* Takashi Fujii,* Joseph A. Dent,† Hajime Fujisawa*,‡ and Shin Takagi†

**Division of Biological Science, Nagoya University Graduate School of Science, Chikusa-ku, Nagoya 464-8602, Japan, †Department of Biology, McGill University, Montreal, Quebec H3A 1B1, Canada and ‡Research Area CREST (Core Research for Evolutional Science and Technology), Japan Science and Technology Corporation, 2-6-15, Shiba Park, Minato-ku, Tokyo 105-0011, Japan*

Manuscript received June 28, 1999
Accepted for publication November 1, 1999

ABSTRACT

The pharynx of *Caenorhabditis elegans* is a neuromuscular organ responsible for feeding, concentrating food by its pumping movement. A class of mutants, the *eat* mutants, are defective in this behavior. We have identified a novel *eat* gene, *eat-20*, encoding a unique transmembrane protein with three EGF motifs. Staining with a specific polyclonal antibody reveals that EAT-20 is expressed predominantly in the pharyngeal muscles and a subset of neurons. Some hypodermal cells also express EAT-20. *eat-20* mutant animals are starved, have smaller brood sizes, and have prolonged egg-laying periods. The starvation apparently results from pharyngeal pumping defects, including a reduced pumping rate and "slippery pumping," in which the contents of the pharynx sometimes move rostrally. However, electrical activity of *eat-20* mutants appears normal by electropharyngeogram.

THE behavior of animals rests on the proper development and function of neuromuscular systems, which in turn requires the proper function of many genes in the nervous system and muscles. Genetics has been an important tool for studying the molecular basis of cell functions and for establishing correlations between cellular function and organismic function.

For understanding the molecular basis of a behavior, the pharynx of *Caenorhabditis elegans* offers several advantages. The behavior of the pharynx is very simple. It consists of two motions, pumping and isthmus peristalsis (Avery and Thomas 1997). These two motions bring food into the pharyngeal lumen and pass it to the intestine. The structure of the pharynx is also very simple. The pharynx is a neuromuscular pump that contains 20 muscles and its own nervous system of 20 neurons (Albertson and Thomson 1976) and is isolated from the rest of the body by basal lamina. The anatomy of each pharyngeal cell has been reconstructed from electron micrographs of serial sections (Albertson and Thomson 1976).

The function of the pharyngeal nervous system has been examined by laser ablation experiments. A motor neuron, M4, is essential for isthmus peristalsis and, consequently, for growth (Avery and Horvitz 1987). Although animals lacking the other 19 pharyngeal neurons retain pumping motions, these other neurons are important for efficient feeding (Avery and Horvitz 1989). In several cases, killing just one type of pharyngeal neuron causes a change in feeding behavior (Avery and Horvitz 1987; Avery 1993b; Raizen *et al.* 1995). The effects of neuron ablations on the electrical activity of the pharyngeal muscles have been also analyzed by electropharyngeogram (EPG; Raizen and Avery 1994).

Combined with these methods, genetical analyses have revealed the functions of individual genes affecting the pharynx. Mutants that show abnormal feeding behavior have been isolated and studied. *eat-4* (Lee *et al.* 1999) affects the function of pharyngeal neurons, and *avr-15* (Dent *et al.* 1997), *eat-5* (Starich *et al.* 1996), and *eat-6* (Davis *et al.* 1995) affect muscle excitability. There may be many genes yet to be identified that are required for development or function of the pharyngeal neuromuscular system.

Here we report the identification and characterization of a novel *eat* gene, *eat-20*, encoding a unique cell membrane protein with EGF motifs. The spatio-temporal pattern of the expression of *eat-20* was examined by reporter-gene expression, *in situ* hybridization, and immunostaining and was found to be primarily in the pharynx. *eat-20* mutants showed slow and slippery pumping and a starved appearance. Defects of *eat-20* mutants in tissues besides the pharynx were also examined.

MATERIALS AND METHODS

Strains: Wild-type worms were *C. elegans* variety Bristol, strain N2. Basic methods for worm culture and genetics were performed as described by Brenner (1974). The transgenic strain carrying the extrachromosomal array *ncEx2* was obtained after coinjection of p5E5 mixed with a transformation marker,

Corresponding author: Shin Takagi, Division of Biological Science, Nagoya University Graduate School of Science, Furo-cho, Chikusa-ku, Nagoya 464-8602, Japan.
E-mail: i45116a@nucc.cc.nagoya-u.ac.jp

pRF4, in a ratio of 3:1, into wild-type hermaphrodites (Mello *et al.* 1991). The strain carrying the integrated transgene array, *ncIs1* LGII, was generated by the irradiation of *ncEx2*-bearing strain with γ-rays. Other strains used in this work are SP273 [*mnDp1(X;V)/ +; mnDf13 X*], DA572 [*eat-4(ad572) III*], DA467 [*eat-6(ad467) V*], DA599 [*eat-8(ad599) III*], DA606 [*eat-10 (ad606)I V*], DA541 [*eat-11(ad541) I*], DA522 [*eat-13(ad522) X*], DA707 [*eat-17(ad707) X*].

Construction and screen of the promoter trap libraries: Promoter trap libraries were constructed and screened as described by Hope (1991) with modifications including the use of *gfp* as a reporter gene. In brief, *C. elegans* genomic DNA prepared from wild-type animals and partially digested with *Sau*3AI was ligated into TU#61 (Chalfie *et al.* 1994). Green fluorescent protein (GFP) expression was examined with a Zeiss (Thornwood, NY) Axioplan microscope using Zeiss filter set 10.

Cloning and sequencing of cDNA and genomic DNA of *eat-20*: Partial determination of the sequence of the insert of p5E5 revealed that the 7-kb insert contains two individual genomic fragments: a 5-kb fragment from LGX and a 2-kb fragment from LGV. The 5-kb fragment at the 3′ side of the insert, which was later shown to include 3-kb upstream to the translation initiation codon and exons 2–8 for the *eat-20* gene, was used for the hybridization probe for cDNA filters. cDNA filters and cDNA clones yk6f1 and yk16h2 were provided by Dr. Yuji Kohara. The 5′ end of the *eat-20* cDNA was amplified by PCR using cDNAs reverse-transcribed from poly(A)$^+$ RNA isolated from mixed-stage wild-type animals as templates. The PCR was performed using the SL1-specific primer SL1ERI (GGAATTC CGTTTAATTACCCAAGTTTGAG) and the gene-specific primer 5E5′3 (GGAATTCGCAACAAACTGCCACATA) using a Gene Amp PCR System 9600 (Perkin Elmer, Norwalk, CT) under the following conditions: 1 cycle at 94° for 20 sec and 35 cycles at 94° for 60 sec, 50° for 120 sec, 68° for 120 sec. DNA sequences were determined for both strands. The nucleotide sequence data reported in this article will appear in the DDBJ/EMBL/GenBank nucleotide sequence databases with the accession nos. AB032748 and AB032749 for *eat-20a* and *eat-20b*, respectively.

EAT-20 antibody production and other immunological methods: The DNA fragment corresponding to nucleotides 359–1281 of the *eat-20* cDNA was cloned into the maltose binding protein (MBP) bacterial expression vector, pMAL-c2 (New England Biolabs, Beverly, MA), and transformed into an *Escherichia coli* strain, BL21 (Figure 1D). The 75-kD fusion protein was purified four times by affinity binding to an amylose resin. A guinea pig (Chubu-kagaku-shizai, Hamamatu, Japan) was immunized primarily with the protein (2 mg) emulsified with Titermax (CytRx) and then with the same amount of the protein emulsified with Freund's incomplete adjuvant (Difco, Detroit) every 2 wk for 6 wk. The serum was absorbed with *E. coli* extract and MBP, and the antibodies were purified by affinity chromatography with the antigen bound to CNBr-activated Sepharose 4B (Pharmacia, Piscataway, NJ).

For immunostaining, worms were freeze-cracked on slides as described by Okamoto and Thomson (1985) and fixed successively with methanol for 5 min and acetone for 5 min at −20°. For the secondary antibody an FITC-labeled goat anti-guinea pig Ig (Amersham, Arlington Heights, IL) diluted with PBST containing 5% skim milk was used. Some specimens were stained with MH27 and Cy3-labeled goat anti-mouse Ig (Amersham) as the primary and secondary antibody, respectively.

GFP expression analysis of *eat-20*: We examined the GFP expression in *ncIs1* hermaphrodites carrying p5E5 as a stable integrated transgenic array. Though p5E5 contains a 2-kb genomic fragment derived from LGV at the 5′ side in addition to the fragment corresponding to the *eat-20* gene, we confirmed that an extrachromosomal array of p5E5 and that of p5E5del, in which the 2-kb fragment was deleted, gave the same GFP expression pattern (data not shown). Thus, the fragment at the 5′ part of the insert had no effects on the expression of GFP. Neurons expressing GFP were first identified in L1 larvae based on the position of their soma according to Sulston *et al.* (1983) and White *et al.* (1986).

***In situ* hybridization of whole-mounted worms:** Digoxigenin (DIG)-11-dUTP-labeled single strand RNA probes were synthesized by using cDNA yk6f1 as a template according to the manufacturer's instructions (Boehringer-Mannheim, Indianapolis). *In situ* hybridization was performed according to Tabara *et al.* (1996).

Isolation of insertion and deletion mutant animals: We performed Tc1 transposon-mediated deletion mutagenesis using the mutator strain MT3126. A Tc1-insertion mutant animal and deletion mutant animals were isolated according to the protocol of Zwaal *et al.* (1993) modified by Dr. Yoshiki Andachi (personal communication).

To detect Tc1 insertion, nested PCR was performed. The first PCR was performed using the two Tc1-specific primers Tc1A (AGCCAGCTACAATGGCTTTC) and Tc1B (GATG CAAACGGATACGCGAC), and the *eat-20* specific primer 5E5-1 (TCTCTTAACGGTGGCTAACC) under the following conditions: one cycle at 94° for 120 sec and 26 cycles of three temperatures (94°, 12 sec; 55°, 12 sec; 72°, 120 sec). The second PCR was performed using the Tc1-specific primers Tc1C (CCAAACAAATCCAGTGCAAC) or Tc1D (TGTCATT TCCTTGCAACCTC), and the *eat-20* specific primer 5E5-2 (CTATCGCTTCGAGGAAGTCG) under the same conditions as the first PCR. To confirm Tc1 insertion, positive pools were examined by PCR, using the *eat-20* specific primer 5E5-3 (TTGTGACATTCGTGGTTGGC) and Tc1A in the first PCR and primers 5E5-5 (ATCACGCTAATGTTCCAAGAAG) and Tc1C in the second PCR. After screening 40,000 animals, we detected and isolated a Tc1-insertion allele, *nc2::Tc1* (Figure 1C).

Since homozygous *eat-20* (*nc2::Tc1*) expressed EAT-20 normally as revealed by immunoblot (Figure 1F) and immunostaining analyses (data not shown), we screened *nc2::Tc1* by PCR in an attempt to detect deletion mutations that arose after imprecise transposon excision (Zwaal *et al.* 1993; Plasterk 1995). DNA pools of *nc2::Tc1*-insertion mutant animals were analyzed by nested PCR using the primers 5E5-1 and 5E5-3 for the first PCR and the primers 5E5-2 and 5E5-5 for the second PCR. Four deletion alleles, *nc3*, *nc4*, *nc5*, and *nc6*, were detected and isolated, and the deleted region for each mutation was determined by PCR and sequence analyses. The mutant animals were outcrossed 10 times to N2.

Pumping assay: Pumping rate was assayed according to Raizen *et al.* (1995).

Trapping and transport of the content of the pharynx was assayed as follows. Several drops of mineral oil were added to a nematode growth medium plate with bacteria. Ten adult worms were transferred to the plate. Pharyngeal pumping was filmed with a Zeiss Axioplan2 microscope, Zeiss 3CCD video camera system ZVS-3C75DE, and a Toshiba videocassette recorder A-J3. The specimen in which the pharynx had only a single droplet of mineral oil was chosen. The movement of a droplet was analyzed by tracing its position in each frame.

Electropharyngeograms: Electropharyngeograms were recorded according to Davis *et al.* (1995).

Measurement of body length: The L4 animals, staged at 40 hr of development according to their vulval morphology (Sulston and Horvitz 1977), were collected and mounted on 4% agar exactly 24 hr later, and their body length was measured by using an image analysis software, IP Lab Spec-

trum (Signal Analytics, Vienna, VA). To assay the body length of starved worms, the L4 animals staged at 40 hr of development were transferred to a bacteria-free plate and body length was measured exactly 24 hr later.

Intestinal autofluorescence: Adult animals, prepared as described in *Measurement of body length*, were observed under an epifluorescent microscope (Axioplan, Zeiss) with the filter system 02.

Egg-laying period: The L4 animals staged at 40 hr of development were picked individually and transferred to fresh plates at 24-hr intervals, and the fertilized eggs laid in a 24-hr period were counted.

Rescue experiments with fosmids: Fosmid H30A04 containing the *eat-20* gene (20 μg/ml) was mixed with the plasmids H20 (20 μg/ml) and Bluescript (160 μg/ml; Stratagene, La Jolla, CA), and was injected into the gonad of mutant animals. H20, which expresses GFP in the entire nervous system, was provided by Dr. Takeshi Ishihara and was used as a transformation marker. The transformants expressing GFP were picked under a fluorescent dissection microscope, MZ APO (Leica).

Complementation tests against *eat-17*: The following results indicated that *eat-20* is distinct from *eat-17*, which was mapped to a similar position on LGX (Figure 1A). First, hermaphrodites *trans*-heterozygous for *nc4* and *eat-17* (*ad707*), or *nc6* and *eat-17* (*ad707*) were indistinguishable from wild-type animals (data not shown). Second, fosmid H30A04 did not rescue the starved appearance of *ad707* (data not shown).

Construction of *nc4/mnDf13* hermaphrodite: *eat-20*(*nc4*) males were crossed to a single hermaphrodite of genotype *mnDp1*(*X;V*)/+: *mnDf13 X*. From plates containing F_1 males, F_1 hermaphrodites younger than the F_1 males were transferred individually to fresh plates and their F_2 progeny were analyzed under a dissection microscope. Because worms homozygous for *mnDp1* are sterile, the F_1's that did not segregate sterile F_2's should have the genotype +/+*V; mnDf13*/*eat-20(nc4) X*. These F_1's had severely starved appearance and produced worms with severely starved appearance, worms with mildly starved appearance, and dead embryos, which are presumably homozygous for *mnDf13*. The phenotypes of 174 F_2 progeny scored were 34 dead embryos, 61 severely starved worms, 45 mildly starved worms, and 34 worms that disappeared during the culture. The worms that disappeared may have left the agar, because some dried-up worms were observed on the wall of the plates. They may be starved worms, which are known to leave agar (Nelson *et al.* 1998). The worms with severely starved appearance were transferred individually and they segregated dead embryos, severely starved worms, and mildly starved worms. Mildly starved worms were indistinguishable from *eat-20*(*nc4*) animals and segregated no dead embryos. Therefore, severely starved worms most likely have the genotype *mnDf13*/*nc4*. To confirm the genotype of F_1 progeny, genomic DNA of F_2 progeny was extracted, and PCR was performed using primers 5E5-1 and 5E5-3. No band corresponding to the wild-type *eat-20* gene was detected.

RESULTS

Mapping of the *eat-20* gene and structural analyses of *eat-20* cDNA: By promoter trapping, we identified a genomic fragment driving expression of reporter *gfp* in the pharynx and a subset of neurons. By sequence analysis, a 5-kb fragment in the insert of promoter trap clone p5E5 was placed on fosmid H30A04 corresponding to the right arm of the X chromosome. The fragment contained a part of a gene and its 5′ flanking region (Figure 1C). We named this gene *eat-20* based on the phenotype caused by the disruption of the gene (see below).

On cDNA filters, the fragment in p5E5 hybridized to cDNA clones yk6f1 and yk16h2. By 5′RACE, we were able to amplify the functional 5′ end of the cDNA using a primer specific to the splicing leader SL1, but not with a primer specific to SL2 (Figure 1B). A comparison of the genomic sequence of H30A04 and the sequences of the cDNAs showed that the *eat-20* gene consisted of 15 exons (including SL1; Figure 1C). *eat-20* is located from nucleotide 6579 to 13,863 of H30A04. In the overlapping region, the sequences of yk6f1 and yk16h2 were identical except that yk16h2 contained 6 extra nucleotides between nucleotides 2253 and 2254. This insertion site corresponded to the 5′ end of exon 13, indicating that the insertion is caused by an alternative splice junction.

The cDNA corresponding to yk6f1 had a single open reading frame encoding a unique polypeptide of 808 amino acid residues (Figure 1B), which we named EAT-20A. EAT-20A has a putative signal sequence (1–20) (von Heijne 1986), three EGF motifs (224–334), a proline-rich region (379–541), an acidic region (542–715), and a hydrophobic region (745–770) (Figure 1, B, D, and E). The presence of a putative N-terminal signal sequence in the predicted protein indicated that the cDNA clone contains the entire coding region. Except for the EGF motifs, no significant homology was found to any other protein. We named the putative product for yk16h2 EAT-20B, in which 2 amino acid residues (VP) were inserted between position 710 and 711 of EAT-20A.

The three EGF motifs were of a noncalcium binding type, and all conserved the 6 consensus cysteine residues. The EGF motifs of EAT-20 were most closely related to those found in Drosophila SLIT (Rothberg *et al.* 1990) and *C. elegans* LIN-12 (Yochem *et al.* 1988) and GLP-1 (Yochem and Greenwald 1989), sharing 38.3, 28.7, and 35.8% amino acid identity, respectively. The proline-rich region contained 27 proline residues out of 163 amino acid residues. The acidic region of 174 residues contained 51 acidic residues of which 39 are glutamate residues. The hydrophobic region of 25 amino acid residues, flanked by basic amino acid residues at the carboxyl side, appears to be a transmembrane domain.

By immunoblot analysis using a specific polyclonal antibody raised against an N-terminal fragment of EAT-20 (Figure 1D), a single band at a position corresponding to the molecular mass of 145 kD was detected in a lysate prepared from wild-type animals of mixed stages (Figure 1F). This size was higher than that predicted for the EAT-20 polypeptide (79 kD), suggesting that the product might be subject to post-translational modifications, such as glycosylation.

EAT-20 expression was observed in the pharynx, neu-

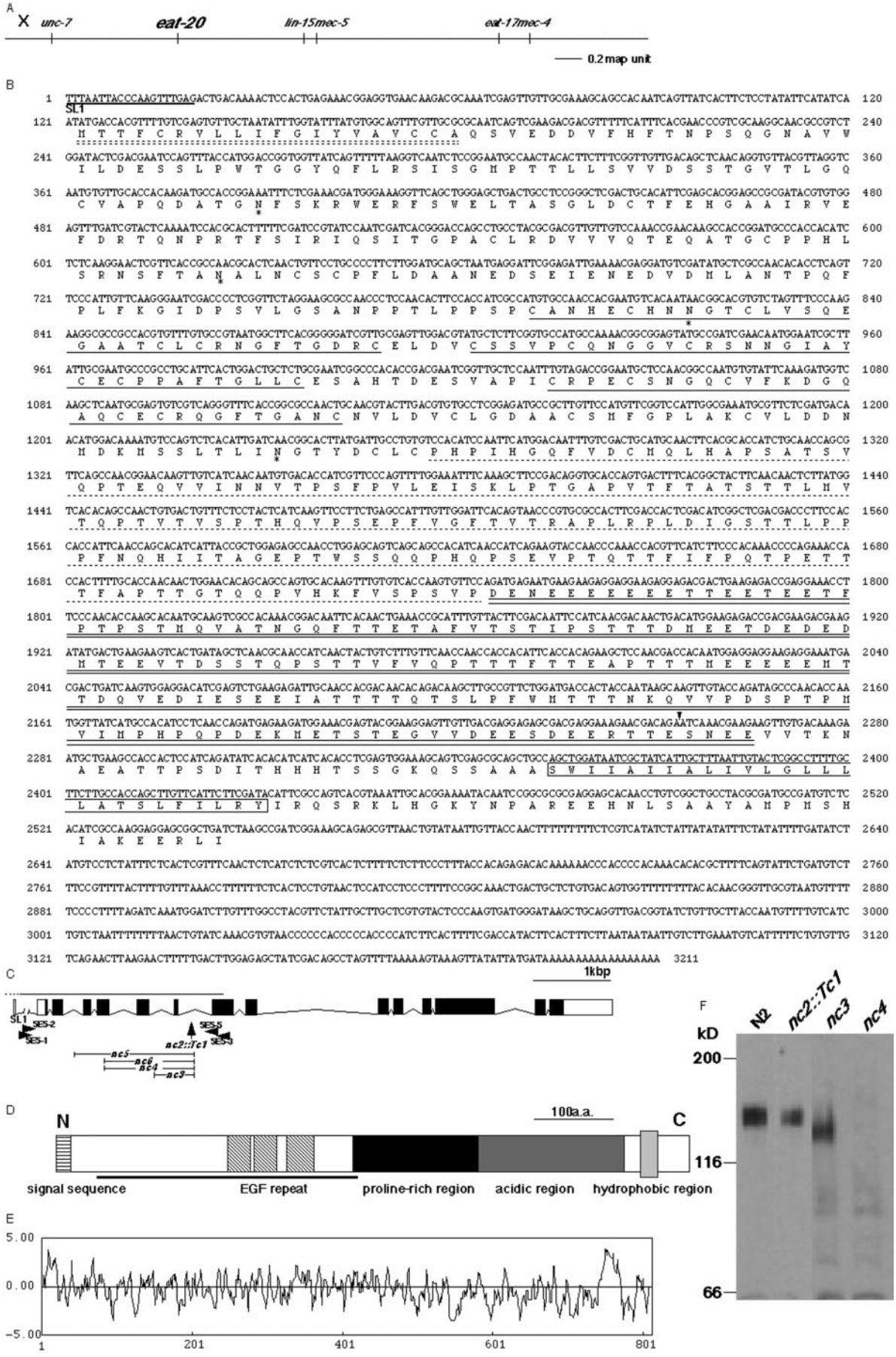
A
X
unc-7
eat-20
lin-15mec-5
eat-17mec-4
0.2 map unit
B
SL1
C
1kbp
SL1
SES-2
SES-1
SES-5
SES-3
nc2::Tc1
nc5
nc6
nc4
nc3
D
N
C
100a.a.
signal sequence
EGF repeat
proline-rich region
acidic region
hydrophobic region
E
5.00
0.00
-5.00
1
201
401
601
801
F
kD
N2
nc2::Tc1
nc3
nc4
200
116
66

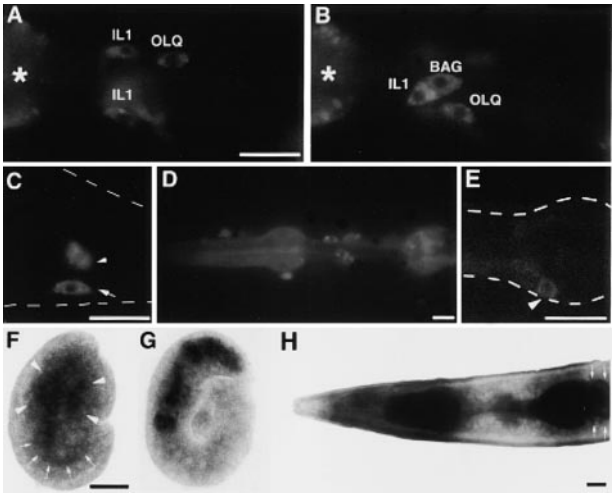

Figure 2.—The *eat-20::gfp* fusion gene and *eat-20* RNA expression in wild-type animals (A–E). The anterior side is to the left and the dorsal side is up. Bars, 10 μm. (A) In the head region of an adult, GFP is expressed in the pharynx (asterisk) and in IL1 and OLQ neurons. (B) The same animal as in A at a different focal plane. BAG, IL1, and OLQ neurons and the pharynx express GFP. (C) In the tail region of an adult, GFP is expressed in the left ALN neuron (arrow) and the right ALN neuron (arrowhead), which is out of the focal plane. The outline of the animal is indicated by a broken line. (D) GFP fluorescence is observed in the procorpus, metacorpus, and terminal bulb of an adult pharynx. (E) GFP fluorescence is observed in I4 at L1. A broken line indicates the pharynx. (F) A 1.5-fold stage embryo. *eat-20* RNA is expressed in the presumptive pharynx (arrowheads) and the intestine (arrows). (G) A threefold stage embryo. *eat-20* RNA is expressed in the pharynx. (H) *eat-20* RNA is expressed in the pharynx, the pharyngeal-intestinal valve (arrows), and some unidentified cells around the pharynx in an adult.

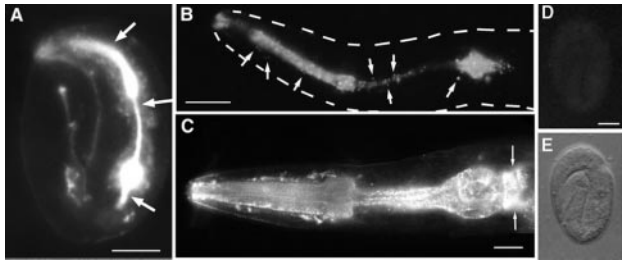

Figure 3.—EAT-20 immunofluorescence in the pharynx. Wild-type animals stained immunofluorescently with the polyclonal antibody against EAT-20. Bars, 10 μm. (A) Threefold stage embryo. Arrows indicate the staining of the lumen of the pharynx. (B) L2 larva. Staining is observed in the lumen of the pharynx. Arrows indicate some of the granular staining in regions surrounding the lumen. (C) L4 larva. EAT-20 protein is expressed in the pharynx. Pharyngeal-intestinal valve (arrows) cells and unidentified circumpharyngeal cells are also stained. (D) *eat-20(nc4)* embryo at the threefold stage. No fluorescent staining is observed. (E) A Nomarski image of the same embryo as in D.

rons, and hypodermal cells: We examined the expression of the *eat-20* gene by using a transgenic line with a *gfp* reporter gene, by immunostaining with the anti-EAT-20 polyclonal antibody, and by *in situ* hybridization against *eat-20* mRNA. The predominant expression of the *eat-20* gene in the pharynx was revealed by all the methods. Expression in part of the nervous system and in hypodermal cells was also detected. *eat-20* was expressed in early embryonic stages and the spatial pattern of the expression changes throughout the development. Details of the expression analysis will be described below.

First, we examined the expression of the *eat-20* gene by using a transgenic line carrying *ncIs1* in which p5E5 was integrated into a chromosome. In embryos, the GFP expression was first detected at the twofold stage. Sometimes eight cells in the anterior half of the body expressed GFP. At the threefold stage, several cells around the pharynx expressed GFP in most embryos. About half of the embryos also expressed GFP weakly in the pharynx. At the first larval stage (L1), GFP was detected

Figure 1.—Molecular structure of *eat-20* and molecular analysis of a Tc1-insertion allele and deletion alleles of *eat-20*. (A) Genetic position of *eat-20* on the right arm of LGX. (B) Sequence analysis of *eat-20*. The sequences for a composite *eat-20* cDNA and the deduced EAT-20 protein are shown with key elements highlighted. A double broken line indicates a signal sequence. EGF motifs are underlined. A broken line indicates the proline-rich region. Double underlining indicates the acidic region. An open box indicates the hydrophobic region. Asterisks indicate potential N-glycosylation sites. cDNA clones yk6f1 and yk16h2 correspond to nucleotide 359-3211 and 89-3200 of the composite cDNA, respectively. An arrowhead indicates the insertion site of 6 bp (TTCCAG) in *eat-20b* cDNA. (C) The gene structure of *eat-20*. The solid and open boxes indicate the exons in the coding region and the noncoding region, respectively. The line above the gene indicates the genomic fragment inserted in clone p5E5. The positions of the Tc1 insertion (*nc2::Tc1*) and deletions (*nc3*, *nc4*, *nc5*, *nc6*) are indicated below the genomic structure of *eat-20*. The nucleotide sequences deleted in the deletion alleles are indicated by bars below the genomic structure. The positions of PCR primers 5E5-1, 5E5-2, 5E5-3, and 5E5-5, which were used to isolate the Tc1-insertion and deletion alleles, are indicated below the genomic structure. The Tc1 insertion is positioned molecularly between nucleotide 8500 and 8501 of fosmid H30A04. *nc3*, *nc4*, *nc5*, and *nc6* mutations delete 494, 1121, 1465, and 1076 nucleotides of the *eat-20* locus, which correspond to nucleotides 8018–8511, 7393–8513, 7039–8503, and 7438–8513 of fosmid H30A04, respectively. The deduced product for *nc3*, *nc4*, *nc5*, and *nc6* would contain 186, 115, 57, and 129 amino residues at the N terminus of EAT-20 followed by GNRPLGSRKRQPSNTSTI AMCQPRMSQ, ESTPRF, ESTPRF, and LESTPRF, respectively. (D) A schematic representation of EAT-20. The fragment used for the immunization is indicated by a bar below the EAT-20 product. (E) A hydropathy profile (Kyte and Doolittle 1982) of EAT-20. (F) A Western blot of the Tc1-insertion and deletion alleles. The positions of molecular mass markers (kD) are indicated at left. In the lanes of *nc3* and *nc4*, the number of animals loaded is increased approximately by five times compared with N2 and *nc2::Tc1*.

in a subset of neurons. About half of the larvae also expressed GFP in the pharynx; expression in the terminal bulb was the most intense. At the adult stage, GFP was detected in the pharyngeal muscles, m3, m4, and m6 (Figure 2D). In addition, GFP was detected in a subset of neurons: IL1, OLQ, BAG, and ALN (Figure 2, A–C), several circumpharyngeal cells (Figure 2D), and coelomocytes (data not shown). Very faint GFP fluorescence was detected in the pharyngeal neurons including I4 and I5 in L1 larvae (Figure 2E).

Next, we examined EAT-20 expression with the anti-EAT-20 polyclonal antibody. Neither immunoblotting (Figure 1F) nor immunostaining analysis (Figure 3E) with the anti-EAT-20 polyclonal antibody detected any signal in *eat-20* mutants (see below), indicating that the following staining is EAT-20 specific. At the 16-cell stage, patches of staining on the entire surface of embryos were first detected. From the comma stage on, staining was detected in coelomocytes, the nervous tissues, hypodermal cells, and the pharynx. At the comma stage, the apical surface of the alimentary canal was stained intensely (Figure 4B) and the basal surface of presumptive pharynx was moderately stained. The staining in the presumptive pharynx gradually weakened thereafter and disappeared completely at the late threefold stage. The staining of the apical surface of the pharynx and pharyngeal intestinal valve remained intense throughout the rest of the embryogenesis stage (Figure 3A). Granular staining in the region surrounding the pharyngeal lumen was observed from the L2 stage on and spread to the external surface (Figure 3B). Staining of the entire surface of the pharyngeal muscle was observed in the late L3 or L4 stage (Figure 3C). The inner linings of the intestine and anus were intensely stained until the twofold stage, and then the staining became weak and disappeared completely at the threefold stage. The anterior-most intestinal cell became stained from the L3 stage (data not shown).

Staining was also observed in the nervous tissues. At the rostral end of the head, staining that seemed to correspond to the distal segments of labial process bundles was seen from the comma stage (Figure 4C) up to the adult stage. In larvae, the staining sometimes extended posteriorly to the level of the isthmus. A pair of cells, which might be support cells of sensory neurons posterior to the distal structures, were stained from the L1 stage up to the adult stage (Figure 4J). The motor neurons in the ventral cord, which sometimes expressed GFP in the promoter trap line, were stained at the early L1 stage (Figure 4F). This staining disappeared at the late L1 stage and, in the later stages, was replaced by segmental staining of the ventral nerve cord. The nerve ring and the nerve bundles that connect the nerve ring and the ventral nerve cord had dots of very faint staining. On the lateral body wall at the base of the tail spike, staining was detected from the L2 stage up to the adult stage, which may correspond to the axon of ALN neuron that expressed reporter GFP in the promoter trap lines (Figure 4H). In the adult male tail, sensory rays were intensely stained (Figure 4I).

There was also extensive hypodermal staining. Weak staining of the seam cells began at the threefold stage

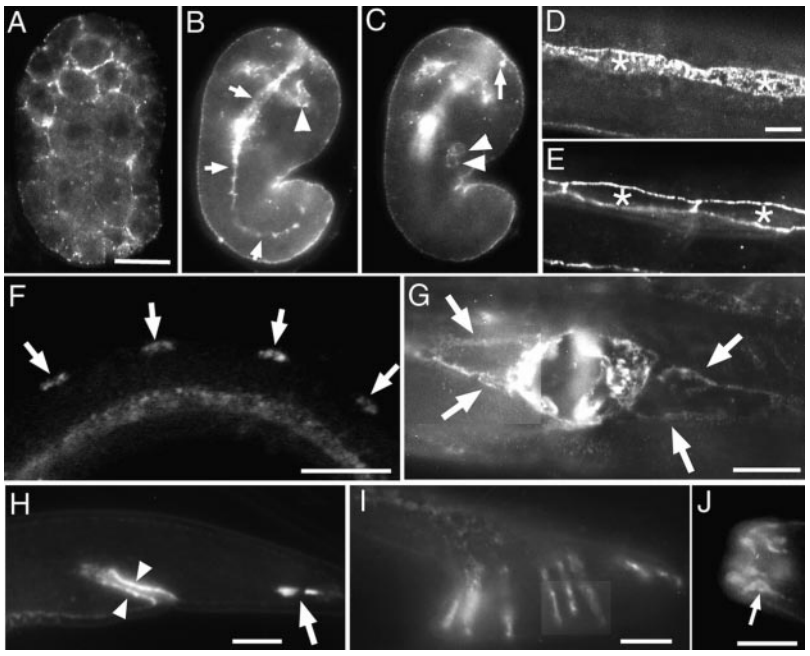

Figure 4.—EAT-20 expression in nonpharyngeal tissues of wild-type animals. Bars, 10 μm. (A) An 88-cell embryo. The surfaces of all the cells are stained. (B) A comma stage embryo. Arrows indicate the digestive tube. An arrowhead indicates an extrapharyngeal cell. (C) The same embryo as in B at a different focal plane. An arrow indicates the tip of a labial process bundle. Arrowheads indicate the coelomocytes. (D and E) Seam cells in an L3 larva. Seam cells are stained with the anti-EAT-20 polyclonal antibody (D) and costained with the monoclonal antibody MH27 to show the cell boundary (E; Hresko *et al.* 1994). Asterisks indicate seam cells. (F) Lateral view of an L1 larva with the anterior side to the right and the ventral side up. Arrows indicate the motor neurons in the ventral cord. A row of seam cells is also stained below. (G) Ventral view of an adult animal showing the staining of the ventral hypodermal ridge and the vulval hypodermis. Arrows indicate the position of the ventral nerve cord in the ventral hypodermal ridge. (H) Lateral view of the tail of an adult hermaphrodite. The anal hypodermis (arrowheads) and a segment of the ALN axon (arrow) are stained. (I) Lateral view of an adult male tail. Sensory rays are stained. (J) Anterior end of a head in an adult. An arrow indicates an unidentified cell posterior to the tip of labial process bundles.

and the staining became intense from the L3 stage up to the adult stage (Figure 4D). Thin longitudinal bands were stained along the dorsal and ventral midline from the rostral end of the body to the base of the tail spike, which corresponds to the position of the dorsal and ventral hypodermal ridges (Figure 4G). The hypodermal staining co-localizing with the position of the ventral nerve cord was the most intense. The hypodermal cells at the opening and inside of the vulva were stained from the L4 stage up to the adult stage (Figure 4G). The hypodermis around the anus was stained from the L2 stage up to the adult stage (Figure 4H). The EAT-20 expression in the seam cells and hypodermal cells is inconsistent with the absence of GFP expression in those cells in the promoter trap lines, suggesting that p5E5 may not contain all the *cis*-regulatory elements necessary for the expression of the *eat-20* gene.

The coelomocytes were continuously stained from the comma stage (Figure 4C) up to the adult stage.

Finally, we examined the expression of the mRNA for *eat-20* by *in situ* hybridization. The signal was first detected in a few cells at the midline of the 1.5-fold stage embryo (Figure 2F). At the twofold stage and thereafter, the signal was detected in the presumptive pharynx (Figure 2G). At the L1 stage, the entire pharynx stained. In the older larvae and adults the entire pharynx stained in some animals though the staining was rather inconsistent. Cells around the metacorpus and the procorpus sometimes stained (Figure 2H).

Screen for mutations of *eat-20*: To analyze the function of EAT-20 *in vivo*, we isolated deletion mutations by using transposon-mediated mutagenesis. First we isolated a Tc1-insertion allele, *nc2::Tc1*, in which a Tc1 inserted in the intron between exons 7 and 8 of *eat-20*. Then we isolated four deletion alleles, *nc3*, *nc4*, *nc5*, and *nc6* (Figure 1C). *nc3*, *nc4*, *nc5*, and *nc6* are expected to lack the C-terminal half of EAT-20 including the EGF motifs. We have detected no abnormality in animals homozygous for *nc2::Tc1* or *nc3*, or in animals of genotype *nc4*/+, *nc5*/+, or *nc6*/+.

Both hermaphrodites and males of *eat-20* mutants were fertile and their locomotion and defecation cycle were normal. They showed no gross morphological defects. Coelomocytes were located in the normal position. When a fluorescent dye, DiI, was injected into the pseudocoelom, they accumulated the dye, indicating that they retained phagocytic activity (data not shown). We could not detect any abnormality in the gross morphology of the nervous system of *nc4* visualized with GFP (data not shown). The pattern of GFP expression by p5E5 in *nc4* was indistinguishable from that in wild-type animals (data not shown).

However, a close examination revealed that animals homozygous for *nc4*, *nc5*, and *nc6* appeared starved (Figure 5, A and B). Compared with wild-type animals, these three alleles exhibited the following phenotypes with similar strength: (1) shorter body length, (2) pale intestine, (3) smaller brood sizes and extended egg-laying periods. The short body length and pale intestine of *eat-20* (*nc4*) were rescued by introduction of fosmid H30A04 containing the wild-type *eat-20* gene (Figure 5D).

Neither immunoblotting (Figure 1F) nor immunostaining analysis (Figure 3E) with the anti-EAT-20 polyclonal antibody detected any signal in animals homozygous for *nc4*, *nc5*, and *nc6*. For *nc3* mutants, a protein was detected by both immunoblotting (Figure 1F) and immunostaining (data not shown), suggesting that *nc3* encodes a truncated EAT-20 protein initiated at a cryptic start site or translated from mRNAs spliced in an abnormal manner, for example by exon-skipping.

To examine the nature of the mutations genetically, we constructed a worm with *eat-20* mutation *in trans* to a deficiency. *mnDf13*/*nc4* hermaphrodites showed more severe starved appearance than *nc4* homozygous animals (Figure 5C). Body length of *mnDf13*/*nc4* was about half of that of wild-type animals. Adult *mnDf13*/*nc4* animals had only a few eggs, whereas most adult *nc4* homozygous animals had >10 eggs. The results raised the possibility that *nc4* is not a null allele (see discussion).

***eat-20* mutants showed starved appearance:** It was reported that abnormal feeding generally causes starved appearance, including a pale intestine and a short and thin body (Avery 1993a). To confirm that *eat-20* mutants are starved, we examined the body size and intestine of the *eat-20* mutant in detail. First, we showed that the body length of 1-day-old adult *nc4* animals was 15% shorter on average than that of wild-type animals of the same stage (Figure 5D). The body length of *nc4* animals gradually increased during the adult stage, but they were consistently smaller than those in the wild-type animals of the corresponding stage. At the L4 stage, body length was shorter in *nc4* animals than in wild-type animals, but the difference was minor (Figure 5D). The duration of each larval stage was not appreciably affected in the mutant animals. Second, to confirm that starvation could have caused this morphological change, we examined the effect of starvation on body length. Wild-type animals were transferred to plates without food at the L4 stage and were examined 24 hr later. Their body length showed little increase from that of L4 larva in the absence of food, whereas that of control well-fed animals increased by 27% on average. The body length of starved wild-type animals is comparable to that of *nc4* animals in the presence of food (Figure 5D). The growth of *nc4* animals was also retarded by starvation, but the degree of retardation was small compared with that of wild-type animals. The distance between the anterior and the posterior turning points of the gonadal arms was also shorter in *nc4* animals (data not shown).

The opacity of the intestine is also an indicator of starvation. When viewed under a dissection microscope, the intestine of wild-type animals and *eat-20* larvae looked dark, whereas that of *nc4* adult animals looked pale. The intestine of *eat-20* L4 animals also sometimes

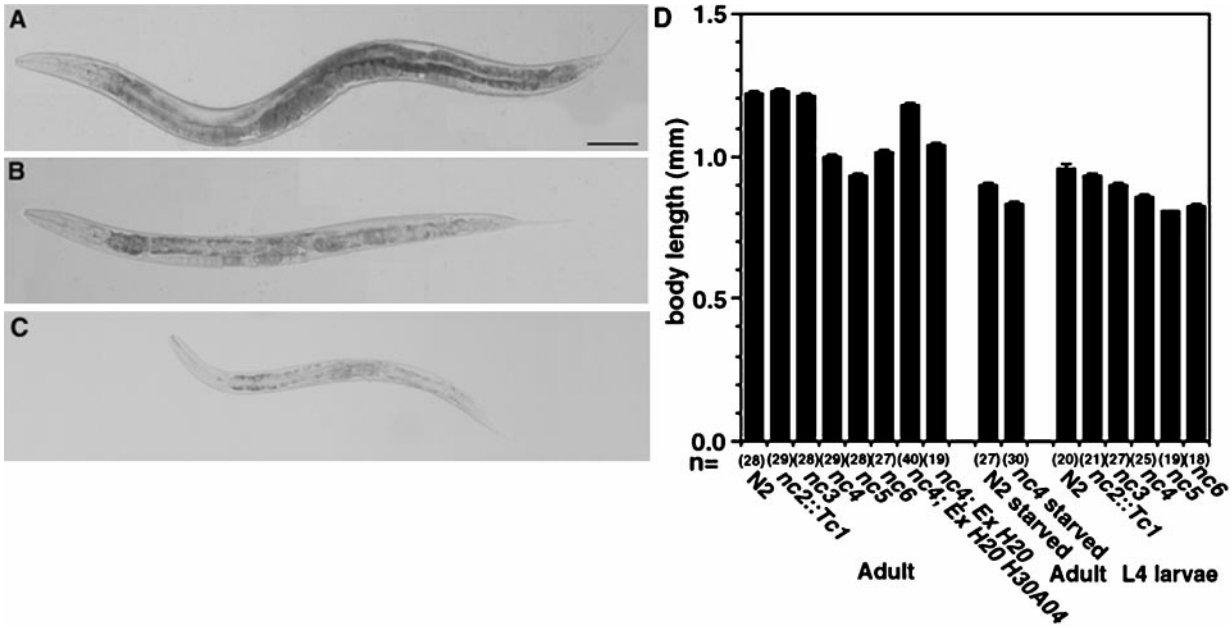

Figure 5.—Body length of *eat-20* mutant animals. Light-transmission microscopic images of a young wild-type adult hermaphrodite (A), an *eat-20(nc4)* hermaphrodite (B), and an *mnDf13*/*nc4* hermaphrodite (C) at the same stage. Bar, 100 μm. (D) Body length of *eat-20* mutant animals at the adult and L4 stage. The body length of *eat-20* mutant animals is smaller at the adult stage, but not appreciably smaller at the L4 stage compared with wild-type animals. Starved adult wild-type animals and *eat-20(nc4)* animals are smaller than well-fed adult wild-type animals and about as long as L4 wild-type animals and adult *eat-20(nc4)* animals. The body length phenotype is rescued by the introduction of the wild-type *eat-20* gene (*nc4; Ex* [*H20, H30A04*]), but not by the transformation marker alone (*nc4; Ex* [*H20*]). The mean body length of each allele is indicated with an error bar indicating SEM. The number of animals examined is indicated below the column (*n*).

looked pale. We presumed that the opacity of the intestine may be related to the quantity of intestinal granules and therefore we examined autofluorescence of intestinal granules by UV irradiation. In wild-type animals, just after the final molt, the intensity of autofluorescence of the intestine increased, whereas in *nc4* animals, autofluorescence was little intensified in the adults (Figure 6, A and B). In weak Eat mutants, such as *eat-4* and *eat-11*, intestinal autofluorescence is indistinguishable from that of wild-type animals, whereas intestinal autofluorescence of medium to strong Eat mutants, such as *eat-6*, *eat-8*, *eat-10*, and *eat-13*, is weak (Figure 6E and data not shown). The adult *eat-20* mutant intestine contained fewer and smaller fluorescent granules than the adult wild-type intestine. The intestinal autofluorescence of starved wild-type animals was weak, lacked bright white granular fluorescence, and looked similar to that of *nc4* animals (Figure 6C). However, the intestines of starved wild-type animals and *nc4* animals were not the same. *nc4* animals had intestines with a normal shape whereas starved wild-type animals had shrunken intestines (Figure 6, C and D).

***eat-20* mutants have abnormal eating behavior:** Though we could not detect any morphological defect in the pharynx by light microscopic observation (data not shown), the starved appearance, which is characteristic of previously isolated Eat mutants defective in feeding (Avery 1993a), prompted us to examine the pharyngeal pumping of *eat-20* mutant animals. We found that pumping rate was reduced in *eat-20* mutant animals by about 15% compared with wild-type animals. Wild-type animals pump 262.1 ± 4.1 times in 1 min, whereas *eat-20*(*nc4*) and *eat-20*(*nc6*) pump 223.4 ± 6.9 and 226.5 ± 6.7 times, respectively.

When worms ingested mineral oil added on the surface of culture, we also found that the posterior transfer of oil droplets in the pharynx was inefficient in *eat-20* mutant animals, a defect similar to what Avery (1993b) called slippery pumping. In the pharynx of wild-type animals, bacteria was swept posteriorly at the beginning of the pump, and during relaxation, the bacteria stayed where they were. On the other hand, bacteria in the slippery pharynx, instead of staying where they are, appear to slip forward during relaxation (Avery 1993b). In *eat-20* mutants, pumping was slippery especially in the isthmus. Once an oil droplet entered the anterior isthmus, it moved back into the metacorpus at a frequency of 1.13 ± 0.34 times during its passage through the isthmus ($n = 16$) in *eat-20*(*nc4*) mutants, which was more than 10 times higher than that in wild-type animals (0.1 ± 0.1 times, $n = 10$, $P = 0.03$). The average time required for transferring a droplet from the anterior metacorpus to the posterior isthmus was significantly longer in *eat-20(nc4)* mutants [1.71 ± 0.21 sec in *eat-20*(*nc4*) and 0.72 ± 0.13 sec in wild-type animals; $P = 0.002$]. Because of the Eat phenotype, we named the

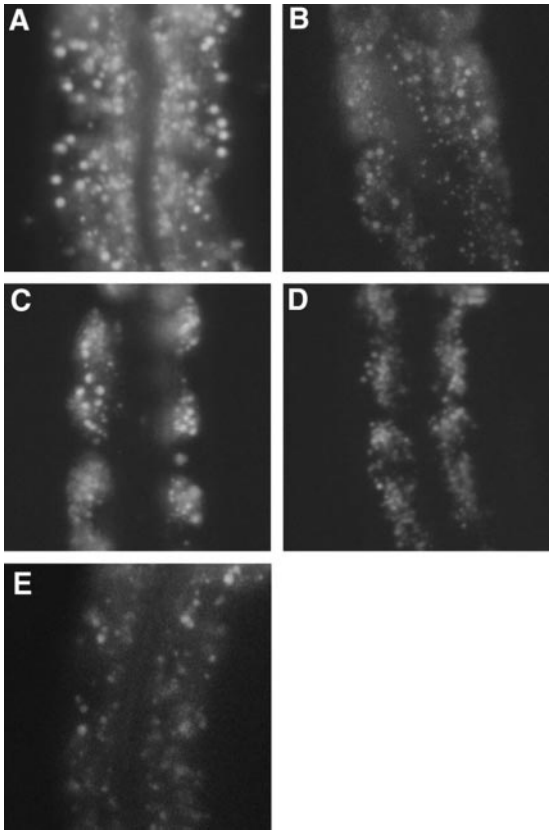

Figure 6.—Weak intestinal autofluorescence of *eat-20* mutant animals. The anterior side is up. (A) In a well-fed wild-type animal, the intensity of autofluorescence of the intestine is strong, and the intestine has many fluorescent granules. (B–E) In a well-fed *eat-20*(*nc4*) animal (B), a starved wild-type animal (C), a starved *eat-20*(*nc4*) animal (D), and a well-fed *eat-13*(*ad522*) animal (E), the intensity of autofluorescence of the intestine is weaker, and there are fewer fluorescent granules than in well-fed wild-type animals.

gene *eat-20*. We have failed to detect any other pharyngeal defects in *eat-20* mutants: the isthmus peristalsis is normal, and contraction of the corpus and terminal bulb are synchronized in *eat-20* mutants. The EPGs of *eat-20* appear to be normal in all respects, including positive transients in the excitation phase, negative transients in the relaxation phase, and M3 inhibitory post synaptic potentials (IPSPs) in the plateau phase (data not shown).

Brood size is reduced and egg-laying period is prolonged in *eat-20* mutants: We found that the brood size of *nc4* animals is 15% smaller than that of wild-type animals (Figure 7A). In addition to reduced brood size, the egg-laying period of *eat-20* mutants was prolonged. Wild-type hermaphrodites start laying eggs after they have reached adulthood. We have counted the number of self-fertilized eggs laid by hermaphrodites at 24-hr intervals by setting the time of the final molt between the L4 stage and the adult stage as day 0. The egg-laying curve showed that wild-type animals laid most of their eggs within the first 3 days with a peak at the second day (Figure 7B). *nc4* animals laid a smaller number of eggs during the period, but kept laying significant numbers of eggs for another several days. Whereas the wild-type egg-laying curves were very stereotypic, those for the mutants showed significant variation among individuals (Figure 7, C and D).

DISCUSSION

By a reverse genetic approach we have identified a novel gene expressed in the pharynx, *eat-20*. The structure of EAT-20 shows that it is a unique example of a cell surface protein encoded by an *eat* gene. We have also characterized the intestinal and reproductive defects of *eat-20* mutants.

***eat-20* encodes a novel protein that acts on the cell surface:** We have revealed that EAT-20 is a novel protein consisting of three EGF motifs, a transmembrane region and an N-terminal signal sequence. The structure indicates that EAT-20 is a cell membrane protein or a secreted protein. The presence of EGF motifs suggests that EAT-20 may interact with other proteins. The EGF motifs of EAT-20 closely resemble those of SLIT (Rothberg *et al.* 1990) in Drosophila, and GLP-1 (Yochem and Greenwald 1989) and LIN-12 (Yochem *et al.* 1988) in *C. elegans*. Although the overall structures of these proteins are not similar, all of them act as a receptor or a ligand for intercellular signaling, and EAT-20 might play a similar role. The fact that the staining with the anti-EAT-20 antibody is localized to the cell surface at sites of cell-cell contact is consistent with this possibility. On the other hand, the expression of EAT-20 is also observed on the cell surface facing the basement membrane, including the basal surface of the pharynx. These expression patterns indicate that a protein(s) that interacts with EAT-20 may be present on the basement membrane as well as on the cell surface.

Although neither immunoblotting nor immunostaining analyses with the anti-EAT-20 polyclonal antibody detected any signal in *nc4*, *nc5*, and *nc6*, there is a possibility that they may not be null alleles because *mnDf13/nc4* animals showed more severe phenotypes than *nc4* homozygous animals. The product of *nc4* might not bind to the anti-EAT-20 antibody, or *nc4* homozygous animals might produce such a small amount of EAT-20 that it was not detected by the antibody. Another possibility is that *nc4* is a null allele, but deletion of unknown genes within *mnDf13* might enhance the starved appearance of *eat-20* mutants because of haploinsufficiency. The isolation and analysis of *eat-20* mutants that have a larger deletion would provide a clue to this problem.

Expression of *eat-20* in the pharynx is likely to be required for proper pumping: We have revealed that pharyngeal pumping is slow and bacterial transport in the isthmus is inefficient in *eat-20* mutants. The reporter gene expression, *in situ* hybridization, and immuno-

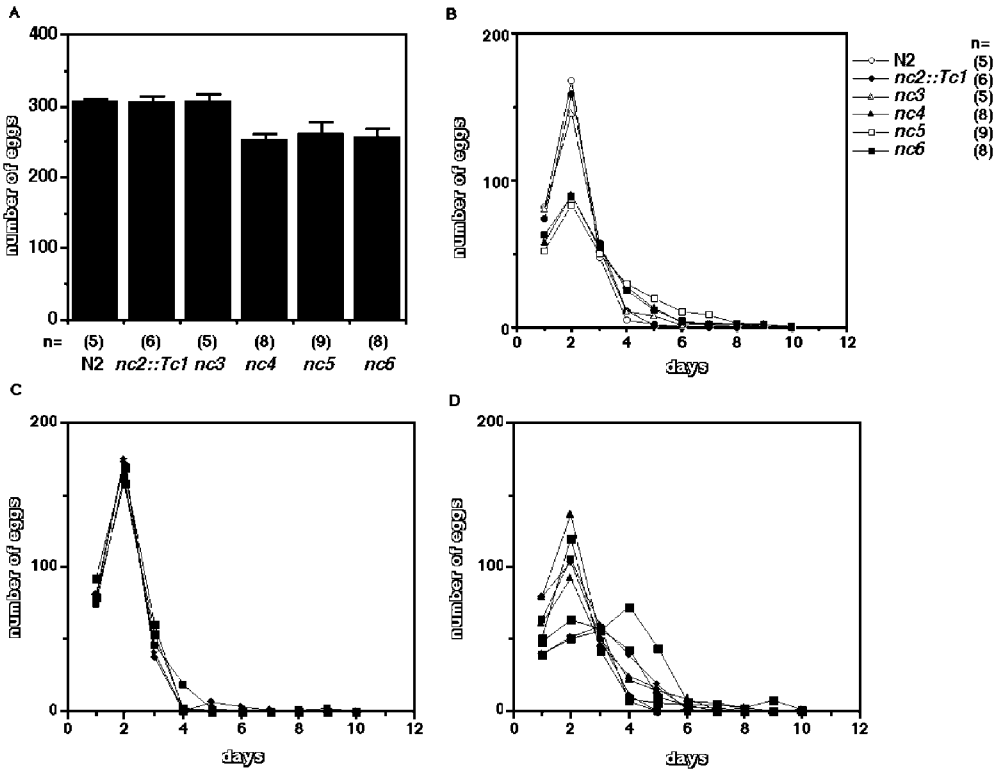

Figure 7.—Reproduction of *eat-20* mutant animals. (A) Brood sizes of *eat-20* mutant animals. The mean of the total number of fertilized eggs laid by a single hermaphrodite is indicated. Error bars indicate SEM. The number of examined animals is indicated below the column (*n*). *eat-20* mutant animals have slightly reduced brood sizes. (B) Egg-laying curves of wild-type and *eat-20* mutant animals. The mean of the total number of eggs laid on each day is indicated. The numbers for wild-type animals are indicated by open circles, for *eat-20* Tc1-insertion mutant (*nc2::Tc1*) animals by solid circles, for *eat-20* deletion mutant (*nc3*, *nc4*, *nc5*, *nc6*) animals by open triangles, solid triangles, open squares, and solid squares, respectively. The number of hermaphrodites examined is indicated (*n*). (C) Egg-laying patterns of five individual wild-type animals are indicated. The number of eggs laid on each day is indicated. (D) Egg-laying patterns of *eat-20*(*nc4*) animals show greater variation. For five individual *eat-20*(*nc4*) animals, the number of eggs laid on each day is indicated.

staining all showed that *eat-20* is expressed in the pharynx. The expression of EAT-20 on the entire surface of the pharyngeal muscle was observed from the L3 or L4 stage. The starved appearance of *eat-20* mutants was first noted in L4 or adult stages, which corresponds to the timing of the pharyngeal expression of EAT-20, indicating that EAT-20 expression in the pharynx from late larval stages on might be important.

The finding that the transport of an oil droplet from the metacorpus to the posterior isthmus in *eat-20* mutants takes ~2.4 times as long as that in wild-type animals indicates that the *eat-20* metacorpus can transport only two-fifths of the food that wild type can transport. This inefficient eating may cause the starved appearance of the *eat-20* mutant, including the reduction in body length.

It has been shown that both neural input and autonomous muscle contractions are required for the proper pumping of the pharynx (Avery and Thomas 1997). The predominant expression of EAT-20 in pharyngeal muscles suggests that these cells may be affected by *eat-20* mutations. However, EPGs of *eat-20* mutants are indistinguishable from those of wild-type animals, indicating that the electrical properties of *eat-20* pharyngeal muscles are normal. Whereas defects in electrical coupling cause unsynchronized contractions in corpus and terminal bulb in *eat-5* mutants (Starich *et al.* 1996), *eat-20* mutants show synchronized pharyngeal contractions. We have failed to detect any gross structural defect in the *eat-20* pharynx.

Alternatively, the *eat-20* mutations might affect pharyngeal neurons. *eat-20* mutants showed slippery pumping in the isthmus, which was also observed in worms whose I5 neuron was killed ($I5^-$ worms) and was even more apparent in $I5^- M3^-$ worms (Avery 1993b). Thus, there is the possibility that the *eat-20* mutations affect I5 or M3. EPGs do not tell whether I5 is affected or not, since electrical events of I5 are not represented in EPGs. However, GFP fluorescence in I5 of the transgenic worms suggests that *eat-20* may have some function in I5. On the other hand, there is no evidence for expression of EAT-20 in M3, and EPGs showed that M3 IPSPs are normal, though it is still possible that M3 of *eat-20* mutants might have a defect that is not detected by EPGs. $I5^- M1^- M2^- M5^- MI^- NSM^-$ worms also exhibit slippery pumping (Avery 1993b). Therefore, EAT-20 might be required in neurons other than M3 in conjunction with I5.

eat-20 mutants also showed slow pumping. Previous reports showed that MC, M2, M3, M4, and NSM are required for maintaining the proper pumping rate (Raizen *et al.* 1995). Pumping rates of $M2^-$, $M3^-$ or NSM^- worms were reduced by about 15% (Raizen *et al.* 1995), which is comparable to that in *eat-20* mutants. M3 IPSPs are normal in *eat-20* mutants, but it is possible that the mutation might affect the pharyngeal muscular motion regulated by M2 or NSM. Since *eat-20* mutants grew to adulthood and showed isthmus peristalsis, M4, which is essential for peristaltic contraction of the isthmus and for growth (Avery and Horvitz 1987), is probably normal. MC neurons appear to be functional in *eat-20* mutants, as the pumping rate of MC^- worms was shown to be much slower than that of *eat-20* mutants. However, the possibility that M4 or MC of *eat-20* mutants might be only partly disabled remains.

Another possibility is that EAT-20 is required in pharyngeal cells other than neurons and muscles whose roles in feeding have been little examined. In summary, at present, the cellular and molecular mechanisms explaining how *eat-20* mutations lead to defective feeding remain open to speculation. Genetic analysis using mosaics or molecular analysis using a cDNA under control of a heterologous promoter to rescue the mutant phenotype would be necessary to determine the primary target of the mutation.

A feeding defect may affect reproduction of *eat-20* mutants: The finding that *eat-20* mutants have a smaller body and a pale intestine is yet another example of the previous observation that the starved appearance is common to mutants affecting pharyngeal function (Avery 1993a). We have strengthened the correlation of feeding defects and starvation by several observations. We found that deprivation of food little affected the growth of *eat-20* L4 larvae whereas it significantly affected the growth of wild-type worms. We have found that *eat-20* intestines not only have a lighter color, but also weaker autofluorescence. Intestinal autofluorescence in mild Eat mutants is indistinguishable from that of wild-type animals, whereas medium to strong Eat mutants have weak intestinal autofluorescence. Thus, weak intestinal autofluorescence is correlated with the severity of the Eat phenotype and is likely to result from a feeding defect. Furthermore, our finding that starved wild-type animals also have weak intestinal autofluorescence points toward a direct connection with feeding. The intestinal phenotypes of *eat* mutants are different from those of *flu* mutants that were previously isolated on the basis of altered intestinal autofluorescence (Babu 1974); *flu* mutants show stronger fluorescence or fluorescence with different colors, whereas *eat* mutants show weak fluorescence, suggesting distinct origins for the defects.

We have revealed that *eat-20* mutants have a smaller brood size and a prolonged egg-laying period. A previous report showed that lower progeny production rates were generally observed in *eat* mutants (Davis *et al.* 1995). Thus, slow reproduction appears to be common to *eat* mutants, and is likely to be a result of feeding defects. In *C. elegans*, yolk proteins are produced by the intestine and transported to the ovary (Kimble and Sharrock 1983). A possible explanation for the reproductive defect is that the intestine of *eat* mutants, because of caloric restriction, might be unable to synthesize enough yolk protein to maintain wild-type rates of oocyte production. Analyses of egg-laying period in previously identified *eat* mutants would help verify this hypothesis.

We are grateful to Dr. Yoshiki Andachi and Dr. Takeshi Ishihara for advice on targeting, Dr. Siegfried Hekimi for critically reading an early version of the manuscript and helpful comments, especially for suggesting that our mutants are Eat, and Mr. Yasunori Murakami for help with antibody analyses. We thank the *C. elegans* Sequencing Consortium for the genomic sequence of H30A04, Dr. Alan Coulson for YAC polytene grids, fosmid H30A04 and H13N06, Dr. Martin Chalfie for TU#61, Dr. Andrew Fire for pPD95.75, Dr. Takeshi Ishihara for H20, Dr. Yuji Kohara for yk6f1, yk16h2g and cDNA filters, Dr. Robert H. Waterston for MH27, and past and present members of our laboratories for advising throughout this work. We appreciate comments of the anonymous reviewers that have improved the manuscript. Some strains were provided by the Caenorhabditis Genetic Center, which is funded by the National Institute for Health National Center for Research Resources. This work was supported by grants from the Ministry of Education, Science, and Culture, Japan (H.F., S.T.) and from the special coordination funds of the Science and Technology Agency of the Japanese Government (H.F., S.T.) and was partly supported by Research Fellowships of the Japan Society for the Promotion of Science for Young Scientist (Y.S.).

Note added in proof: Because *eat-20(nc4)* may not be a null allele, we have examined the possibility that *nc4* would be a hypomorphic allele of a known gene. As *mnDf43* complemented *nc4*, *nc4* was placed in the interval between the right bleak point of *mnDf43* and *lin-15*. We have performed a complementation test against the known *let* mutations mapped to the region. *let-15(m127)*, *let-18(mn122)*, *let-38(mn141)*, and *let-40(mn150)* all complemented *nc4*, suggesting that *nc4* is not an allele of these genes.

LITERATURE CITED

Albertson, D. G., and J. N. Thomson, 1976 The pharynx of *C. elegans*. Philos. Trans. R. Soc. Lond. B Biol. Sci. **275:** 299–325.

Avery, L., 1993a The genetics of feeding in *Caenorhabditis elegans*. Genetics **133:** 897–917.

Avery, L., 1993b Motor neuron M3 controls pharyngeal muscle relaxation timing in *Caenorhabditis elegans*. J. Exp. Biol. **175:** 283–297.

Avery, L., and H. R. Horvitz, 1987 A cell that dies during wild-type *C. elegans* development can function as a neuron in a *ced-3* mutant. Cell **51:** 1071–1078.

Avery, L., and H. R. Horvitz, 1989 Pharyngeal pumping continues after laser killing of the pharyngeal nervous system of *C. elegans*. Neuron **3:** 473–485.

Avery, L., and J. H. Thomas, 1997 Feeding and defecation, pp. 679–716 in *C. elegans II*, edited by D. L. Riddle, T. Blumenthal, B. J. Mayer and J. R. Priess. Cold Spring Harbor Laboratory Press, Cold Spring Harbor, NY.

Babu, P., 1974 Biochemical genetics of *C. elegans*. Mol. Gen. Genet. **135:** 39–44.

Brenner, S. 1974 The genetics of *Caenorhabditis elegans*. Genetics **77:** 71–94.

Chalfie, M., Y. Tu, G. Euskirchen, W. W. Ward and D. C. Prasher,

1994 Green fluorescent protein as a marker for gene expression. Science **263:** 802–805.

Davis, M. W., D. Somerville, R. Y. Lee, S. Lockery, L. Avery *et al.*, 1995 Mutations in the *Caenorhabditis elegans* Na,K-ATPase alpha-subunit gene, *eat-6*, disrupt excitable cell function. J. Neurosci. **15:** 8408–8418.

Dent, J. A., M. W. Davis and L. Avery, 1997 *avr-15* encodes a chloride channel subunit that mediates inhibitory glutamatergic neurotransmission and ivermectin sensitivity in *Caenorhabditis elegans*. EMBO J. **16:** 5867–5879.

Hope, I. A., 1991 Promoter trapping in *Caenorhabditis elegans*. Development **113:** 399–408.

Hresko, M. C., B. D. Williams and R. H. Waterston, 1994 Assembly of body wall muscle and muscle cell attachment structures in *Caenorhabditis elegans*. J. Cell Biol. **124:** 491–506.

Kimble, J., and W. J. Sharrock, 1983 Tissue-specific synthesis of yolk proteins in *Caenorhabditis elegans*. Dev. Biol. **96:** 189–196.

Kyte, J., and R. F. Doolittle, 1982 A simple method for displaying the hydropathic character of a protein. J. Mol. Biol. **157:** 105–132.

Lee, R. Y. N., E. R. Sawin, M. Chalfie, H. R. Horvitz and L. Avery 1999 EAT-4, a homolog of a mammalian sodium-dependent inorganic phosphate cotransporter, is necessary for glutamatergic neurotransmission in *Caenorhabditis elegans*. J. Neurosci. **19:** 159–167.

Mello, C. C., J. M. Kramer, D. Stinchcomb and V. Ambros, 1991 Efficient gene transfer in *C. elegans*: extrachromosomal maintenance and integration of transforming sequences. EMBO J. **10:** 3959–3970.

Nelson, L. S., M. L. Rosoff and C. Li, 1998 Disruption of a neuropeptide gene, *flp-1*, causes multiple behavioral defects in *Caenorhabditis elegans*. Science **281:** 1686–1690.

Okamoto, H., and J. N. Thomson, 1985 Monoclonal antibodies which distinguish certain classes of neuronal and supporting cells in the nervous tissue of the nematode *Caenorhabditis elegans*. J. Neurosci. **5:** 643–653.

Plasterk, R. H. A., 1995 Reverse genetics: from gene sequence to mutant worm, pp. 59–80 in *Methods in Cell Biology. Caenorhabditis elegans: Modern Biological Analysis of an Organism*, edited by H. F. Epstein and D. C. Shakes. Academic Press, San Diego.

Raizen, D. M. and L. Avery, 1994 Electrical activity and behavior in the pharynx of *Caenorhabditis elegans*. Neuron **12:** 483–495.

Raizen, D. M., R. Y. Lee and L. Avery, 1995 Interacting genes required for pharyngeal excitation by motor neuron MC in *Caenorhabditis elegans*. Genetics **141:** 1365–1382.

Rothberg, J. M., J. R. Jakobs, C. S. Goodman and S. Artavanis-Tsakonas, 1990 *slit*: an extracellular protein necessary for development of midline glia and commissural axon pathways contains both EGF and LRR domains. Genes Dev. **4:** 2169–2187.

Starich, T. A., R. Y. Lee, C. Panzarella, L. Avery and J. E. Shaw, 1996 *eat-5* and *unc-7* represent a multigene family in *Caenorhabditis elegans* involved in cell-cell coupling. J. Cell Biol. **134:** 537–548.

Sulston, J. E., and H. R. Horvitz, 1977 Post-embryonic cell lineages of the nematode, *Caenorhabditis elegans*. Dev. Biol. **56:** 110–156.

Sulston, J. E., E. Schierenberg, J. G. White and J. N. Thomson, 1983 The embryonic cell lineage of the nematode *Caenorhabditis elegans*. Dev. Biol. **100:** 64–119.

Tabara, H., T. Motohashi and Y. Kohara, 1996 A multi-well version of in situ hybridization on whole mount embryos of *Caenorhabditis elegans*. Nucleic Acids Res. **24:** 2119–2124.

von Heijne, G., 1986 A new method for predicting signal sequence cleavage site. Nucleic Acids Res. **14:** 4683–4690.

White, J. G., E. Southgate, J. N. Thomson and S. Brenner, 1986 The structure of the nervous system of the nematode *C. elegans*. Philos. Trans. R. Soc. Lond. B Biol. Sci. **314:** 1–340.

Yochem, J., and I. Greenwald, 1989 *glp-1* and *lin-12*, genes implicated in distinct cell-cell interactions in *C. elegans*, encode similar transmembrane proteins. Cell **58:** 553–563.

Yochem, J., K. Weston and I. Greenwald, 1988 The *Caenorhabditis elegans lin-12* gene encodes a transmembrane protein with overall similarity to *Drosophila* Notch. Nature **335:** 547–550.

Zwaal, R. R., A. Broeks, J. van Meurs, J. T. Groenen and R. H. Plasterk, 1993 Target-selected gene inactivation in *Caenorhabditis elegans* by using a frozen transposon insertion mutant bank. Proc. Natl. Acad. Sci. USA **90:** 7431–7435.

Communicating editor: R. K. Herman